Official journal of the American Society of Gene & Cell Therapy

MTOpen

Contributions of Mouse and Human Hematopoietic Cells to Remodeling of the Adult Auditory Nerve After Neuron Loss

Hainan Lang[1], Eishi Nishimoto[1], Yazhi Xing[1], LaShardai N Brown[1], Kenyaria V Noble[1], Jeremy L Barth[2], Amanda C LaRue[1,3], Kiyoshi Ando[4] and Bradley A Schulte[1]

[1]Department of Pathology and Laboratory Medicine, Medical University of South Carolina, Charleston, South Carolina, USA; [2]Department of Regenerative Medicine and Cell Biology, Medical University of South Carolina, Charleston, South Carolina, USA; [3]Research Services, Ralph H. Johnson Department of Veterans Affairs Medical Center, Charleston, South Carolina, USA; [4]Research Center for Regenerative Medicine, Division of Hematopoiesis, Tokai University School of Medicine, Tokyo, Japan

The peripheral auditory nerve (AN) carries sound information from sensory hair cells to the brain. The present study investigated the contribution of mouse and human hematopoietic stem cells (HSCs) to cellular diversity in the AN following the destruction of neuron cell bodies, also known as spiral ganglion neurons (SGNs). Exposure of the adult mouse cochlea to ouabain selectively killed type I SGNs and disrupted the blood-labyrinth barrier. This procedure also resulted in the upregulation of genes associated with hematopoietic cell homing and differentiation, and provided an environment conducive to the tissue engraftment of circulating stem/progenitor cells into the AN. Experiments were performed using both a mouse-mouse bone marrow transplantation model and a severely immune-incompetent mouse model transplanted with human CD34$^+$ cord blood cells. Quantitative immunohistochemical analysis of recipient mice demonstrated that ouabain injury promoted an increase in the number of both HSC-derived macrophages and HSC-derived nonmacrophages in the AN. Although rare, a few HSC-derived cells in the injured AN exhibited glial-like qualities. These results suggest that human hematopoietic cells participate in remodeling of the AN after neuron cell body loss and that hematopoietic cells can be an important resource for promoting AN repair/regeneration in the adult inner ear.

Received 24 May 2016; accepted 25 August 2016; advance online publication 4 October 2016. doi:10.1038/mt.2016.174

INTRODUCTION

The degeneration of various cell types in the organ of Corti and auditory nerve (AN) is a key cause of peripheral hearing loss. Unlike spiral ganglion neurons (SGNs, neuronal cells of the AN) and sensory hair cells, which are unable to regenerate, glial cells in the AN and fibrocytes in the spiral ligament (which is located in the lateral wall of the cochlear duct) share the ability to repopulate after ototoxic drug exposure or noise-induced injury.[1–3] A growing body of evidence suggests that highly specialized glial cells in the AN, subpopulations of fibrocytes in the cochlear spiral ligament and macrophages play important roles both in maintaining normal auditory physiology and in repairing damage in pathological conditions.[4–11] However, the mechanisms whereby glial cells and other nonsensory cells are able to regenerate in the adult inner ear remain unknown. It is well-established that bone marrow-derived stem cells have the potential to differentiate into multiple nonhematopoietic cell lineages and can contribute to tissue homeostasis and repair in various organs.[12–16] Our previous studies have documented that fibrocytes in the cochlear lateral wall of adult mice are continually derived from bone marrow cells, more specifically, from hematopoietic stem cells (HSCs).[17] Here, we investigated the possible contribution of HSCs to repair and regenerative processes in the injured AN.

Ouabain is a cardiac glycoside that inhibits Na,K-ATPase activity. It has been used as a blocking agent to study the functional role of Na,K-ATPase in inner ear fluid and ion homeostasis.[18–20] Application of ouabain to the round window of gerbils and mice results in a rapid and highly selective elimination of type I SGNs without degeneration of cells within the organ of Corti, the strial vascularis and spiral ligament in the cochlear lateral wall.[3,21,22] Here, we used this approach to investigate the effects of acute injury on tissue engraftment of mouse and human hematopoietic cells in the adult AN using a mouse-mouse bone marrow transplantation model and a human-mouse hematopoietic cell transplantation model. The mouse-mouse model of bone-marrow transplant was established by injecting green fluorescent protein positive (GFP$^+$) HSCs into adult irradiated adult mice.[17]

The ability to perform studies with human stem cells *in vivo* is limited by ethical and technical constraints. To overcome these limitations, we employed a human-mouse transplantation model (humanized mice) based on immunodeficient mice to evaluate the tissue engraftment and differentiation of human HSCs to the adult inner ear after ouabain exposure.[23–25] NOD.Cg-Prkdc^{scid} IL2rg^{tm1Wjl}/Szj (NSG) mice are deficient in mature lymphocytes, lack detectable serum Ig, and have low natural killer cell activity. These mice do not develop thymic lymphoma, have a long

This work was performed in Charleston, South Carolina, USA.

Correspondence: Hainan Lang, Department of Pathology and Laboratory Medicine, Medical University of South Carolina, 165 Ashley Avenue, PO BOX 250908, Charleston, South Carolina 29425, USA. E-mail: langh@musc.edu

lifespan and have proven to be superior to other immunocompromised models for supporting tissue engraftment of human hematopoietic cells.[25,26] In this study, NSG mice were preconditioned with irradiation and transplanted with human CD34$^+$ cells isolated from cord blood for the examination of hematopoietic cell engraftment and differentiation in the injured AN.

Macrophages and microglia, the resident immune cells in the brain, are recruited to regions of degenerative neural tissues under many pathological conditions and play important roles in regulating not only neural cell death but also the survival, proliferation and differentiation of neural stem/progenitor cells.[27] Recruitment of bone marrow-derived microglial/macrophages into nervous tissues has been reported during postnatal development[28–30] and in several pathological conditions in adult brain.[31,32] Bone marrow-derived macrophage infiltration also has been demonstrated in cochlear tissues following exposure to noise and ototoxic drugs.[9,33] In this study, we have evaluated the extent to which mouse bone marrow-derived and human HSC-derived macrophages respond to AN injury using both the mouse-mouse and the human-mouse transplantation models.

RESULTS

Tissue engraftment of mouse bone marrow-derived cells in injured AN

We evaluated the contribution of HSC-derived cells to nerve repair/plasticity and microenvironment alterations in the adult AN after injury using a well-established bone marrow transplantation model.[17,28,34] Un-manipulated GFP$^+$ bone marrow (BM) mononuclear cells isolated from transgenic C57BL/6-Ly5.2 were transplanted into 3-month-old C57BL/6-Ly5.1 mice preconditioned with a single 950-cGy dose of total body irradiation (**Figure 1a**). This approach resulted in robust long-term reconstitution of hematopoiesis with GFP$^+$ peripheral blood cell progeny at a high level of multi-lineage engraftment (ranging from 49 to 96%) at 8–26 months post-transplantation. **Figure 1b** shows the reconstitution of GFP$^+$ peripheral blood in a representative recipient mouse 8 month after transplantation. Similar to our earlier studies using CBA/CaJ mice[39], ouabain promoted about 80–90% loss of neuronal cells 3 days after exposure (**Figure 1c**). GFP$^+$ BM-derived cells were increased significantly in the injured AN at 7 days after ouabain exposure (**Figure 1d,e**).

Ultrastructural alterations in the injured adult AN

Similar to the blood–brain barrier in the central nervous system, the blood–labyrinth barrier (BLB) in the inner ear acts as a critical physiological barrier regulating the selective transport of macromolecules and ions and maintaining cochlear ion homeostasis.[35,36] It is well known that bone marrow-derived cells are preferentially recruited to lesioned regions of the brain through the blood–brain barriers and differentiate into microglia that comprise the resident phagocytes of the central nervous system.[37,38] Nonfenestrated capillaries with well-developed tight and adherens junctions between adjacent endothelial cells are a key element of the BLB. To evaluate the effects of acute injury on the disruption of the BLB and the surrounding environment, we examined ultrastructural alterations in the CBA/CaJ mouse AN after ouabain exposure. Ultrastructural examination of ouabain-treated ANs revealed selective degeneration of type I SGNs 3 days after exposure (**Figure 2c,d**), validating results shown in our immunohistochemical analysis (**Figure 1c**) and supporting our previous observations.[39] Activated macrophages were seen closely associated with and in some cases encapsulating degenerative SGNs (**Figure 2c,d**) and were also frequently observed adjacent to capillaries (**Figure 2j**). As shown in **Figure 2f,g**, capillary endothelial cells in the AN of normal young adult mice, were joined by normal appearing junctional complexes. However, following ouabain exposure, the apical surface of capillary endothelial cells developed a scalloped appearance in the smooth luminal surface not normally seen in the smooth luminal surface of uninjured endothelial cells (**Figure 2e** and **Figure 2h–j**). Other BLB abnormalities included the appearance of small vesicles in the cytoplasm of endothelial cells and the separation of the overlapping endothelial cell processes by an electron-lucent substance. Platelet endothelial cell adhesion molecule-1 (CD31), a 140 kDa type I integral membrane glycoprotein, is highly expressed on mature endothelial cells. Immunostaining for CD31 antibody was performed in control (**Figure 2k**) and ouabain-exposed ANs (**Figure 2l**) and revealed markedly dilated capillaries 3 days after ouabain exposure. The average diameters of CD31$^+$ vessels are 2.40 ± 0.25 and 7.42 ± 0.89 μm for the controls and ouabain treated nerves, respectively (data were presented as mean ± standard error of the mean; $n = 12$ for the controls and $n = 13$ for the ouabain-treated group; $P = 9.30016\text{E}{-}05$; $t = 5.219$; Student's unpaired t-test).

Ouabain injury stimulates expression of genes associated with HSC homing and macrophage activation in the AN

To investigate molecular changes associated with AN injury that may influence tissue distribution and engraftment of BM-derived cells, we examined mRNA expression levels of genes linked to HSC differentiation and homing using our previously reported microarray data (NCBI Gene Expression Omnibus; GSE59417) obtained from ouabain-treated ANs from adult CBA/CaJ mice.[40] This analysis revealed 180 genes that were differentially expressed at either 3 or 7 days following ouabain exposure (**Figure 3a**; **Supplementary Table S1**). Seventy-three percent of these genes (131/180) were upregulated after ouabain injury. **Figure 3b** shows expression profiles for six representative up-regulated genes including C-C chemokine receptor type 2 (Ccr2), C-X-C motif chemokine 12 (Cxcl12, also termed as stromal cell-derived factor 1 (SDF-1)), C-X-C motif chemokine receptor 4 (Cxcr4), protein tyrosine phosphatase receptor type C (Ptprc, also known as CD45, leukocyte common antigen), vascular cell adhesion molecule-1 (Vcam1) and runt-related transcription factor 2 (Runx2). The role of these genes in HSC migrating and homing in injured tissue has been well-documented[41–46]

Since HSCs are capable of giving rise to differentiated microglia/macrophages,[28–30] we examined the expression of genes related to macrophage/microglia activity. This evaluation identified 164 genes that were differentially expressed following ouabain injury (**Figure 3c**; **Supplementary Table S2**). The majority of these genes (75%; 123/164) were upregulated in response to the injury and several of the upregulated genes were linked to macrophage activation, including the C-C motif chemokine ligand 2 (Ccl2), C-C

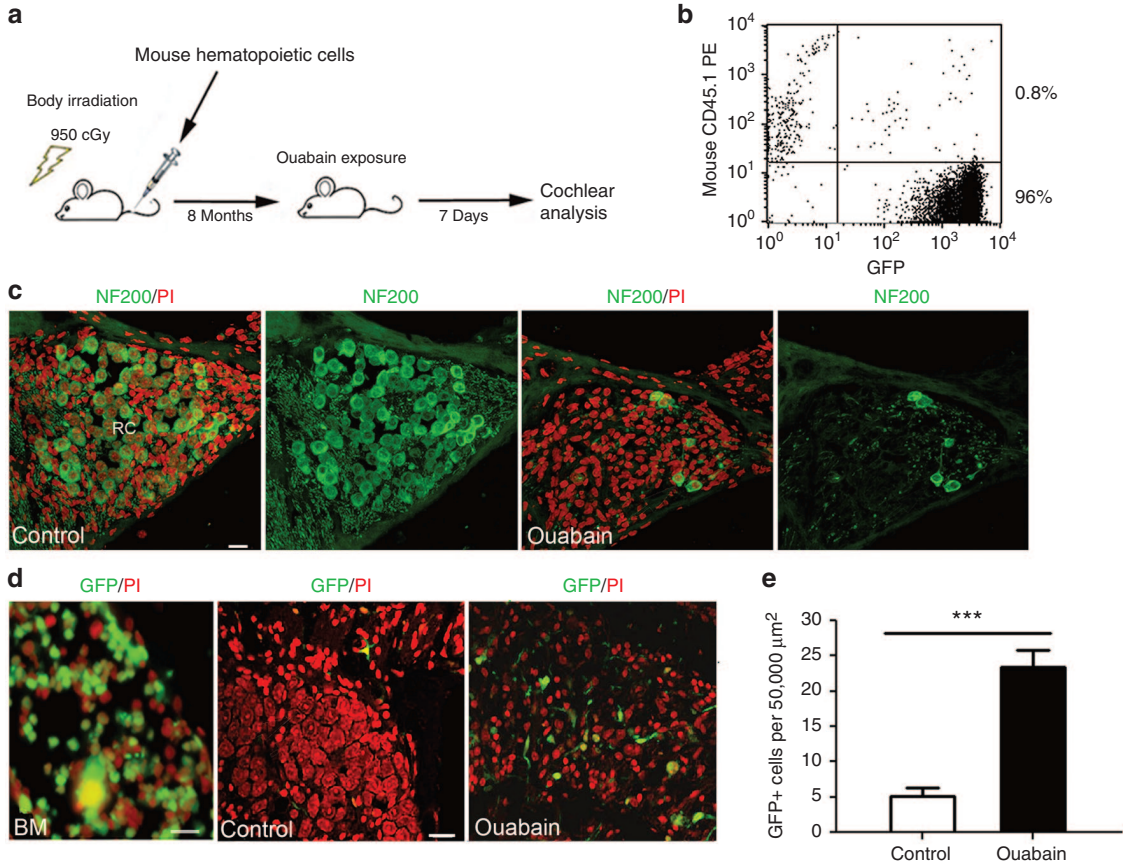

Figure 1 Enhanced tissue engraftment and differentiation of mouse bone marrow-derived cells in the ouabain-treated AN. (**a**) Experimental approach for mouse hematopoietic cell implantation and selective deletion of neuronal cells in AN. (**b**) Flow cytometric analysis of nucleated blood cells demonstrates robust engraftment (about 96%) in peripheral blood from a representative recipient C57BL/6-Ly5.1 mouse 8 months after bone marrow transplantation. (**c**) Anti-neurofilament 200 (NF200) staining shows that only a few SGNs remain in Rosenthal's canal (RC) at 3 days after ouabain exposure. (**d**) The left panel shows that a majority of cells in bone marrow (BM) of recipient mice are derived from transplanted GFP⁺ cells. The number of transplanted GFP⁺ BM-derived cells in the spiral ganglion was greatly increased 7 days after ouabain injury. (**e**) Quantitative analysis indicated a significant increase in GFP⁺ cells in the AN 7 days after ouabain exposure (**$P < 0.01$; data were presented as mean ± SEM; $n = 3$ mice per condition; $P = 0.0003$; $t = 11.56$; unpaired t-test). Scale bars, 10 µm in **c** and **b**.

motif chemokine ligand 3 (Ccl3), CX3C chemokine receptor 1 (Cx3cr1), transforming growth factor beta 1 (Tgfb1), transforming growth factor beta 2 (Tgfb2), and Toll-like receptor 2 (Tlr2) (**Figure 3d**). Additionally, numerous upregulated genes were well known macrophage/microglia markers, including allograft inflammatory factor 1 (Aif1, also known as ionized calcium-binding adapter molecule 1; Iba-1), EGF-like module-containing mucin-like hormone receptor-like 1 (Emr1/Adgre1, also known as F4/80), integrin alpha M (Itgam, also known as CD11b), and transforming growth factor beta 3 (Tgfb3) (**Figure 3e**).

Ouabain injury stimulates macrophage infiltration of the AN

To investigate if upregulation of genes associated with macrophage activation leads to increased macrophage infiltration in the injured AN, Iba-1⁺ macrophages were quantified in the AN at 3 and 7 days after ouabain exposure. As shown in **Figure 4b,c**, macrophage numbers were increased significantly throughout the cochlear duct 3 days after ouabain exposure. The morphology of macrophages/microglia often indicate their cellular physiological state. Amoeboid or rounded macrophages indicates reactive or engulfment functions while ramified, or highly branched macrophages point to surveillance or sentry roles.[47] The majority of these infiltrating Iba-1⁺ macrophages had the appearance of activated amoeboid cells with large round shapes, while macrophages in the control ANs were normally present in the inactive ramified form (**Figure 4b**).

Macrophages and non-macrophages observed in the injured AN arise from HSCs

To determine if infiltrating macrophages observed in the ouabain-exposed ANs arose from migrated HSCs, we examined engrafted cells in the cochleae of ouabain-injured BM transplanted mice. Dual immunostaining was performed for the transplanted cell marker GFP and several macrophage markers that have been used previously in rodent cochlear tissues including CD45, F4/80 and Iba-1.[9,17,33,48,49] **Figure 4d–g** illustrates that GFP⁺ BM-derived cells can differentiate into both macrophage and nonmacrophage phenotypes in the ouabain-exposed AN. In a previous study we showed that Sox2⁺ glial cells were increased in the AN 3 days after ouabain exposure.[39] To determine if BM-derived cells contributed to the Sox2⁺ glial cell population, dual immunostaining for GFP⁺

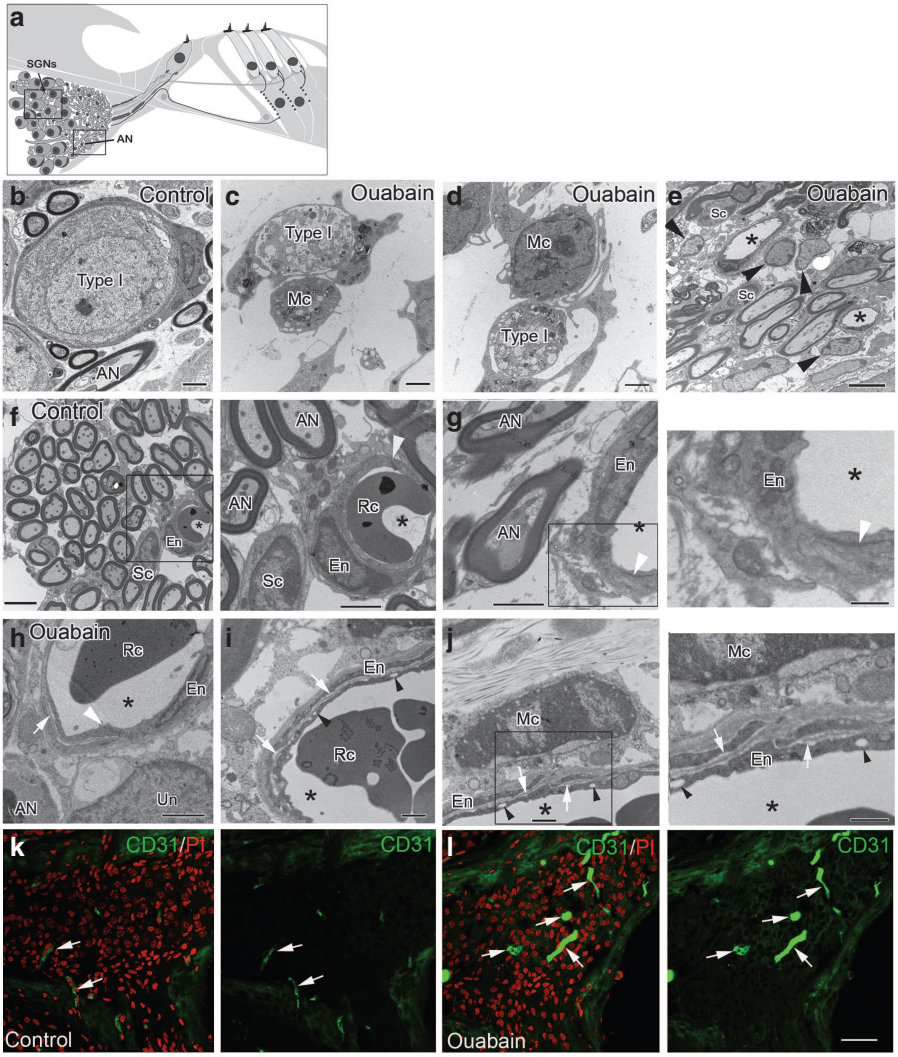

Figure 2 Changes in the microvasculature and macrophage infiltration in the AN after ouabain exposure. (**a**) Illustration showing regions of AN fibers (boxed areas) corresponding to areas where images of AN neuronal cells (also name as spiral ganglion neurons, SGNs; **b–d**) and AN fibers (AN, **e–j**) were taken. (**b**) Normal type I (Type I) SGN from a control mouse. (**c,d**) Three days after ouabain treatment degenerate type I SGNs are closely juxtaposed to macrophages (Mc). (**e**) Several glia-like cells (arrowheads) appeared around microvasculature in Rosenthal's canal of the ouabain-treated ear. (**f,g**) Normal appearance of AN fibers and microvasculature in Rosenthal's canal. The right panels of **f** and **g** show magnified images of the boxed areas in **f** and **g,** respectively. Endothelial cells (En) are joined by normal appearing tight junctions (white arrowheads). Asterisks indicate capillary lumens. Red blood cell; Rc. (**h–j**) Pathological alterations in the microvasculature were seen in the ouabain treated ANs. Right panel of **j** is a magnified image of the boxed area in **j**. Capillary lumens (asterisks) were expanded and the normally smooth apical surface of endothelial cells was crenulated. Clear vesicles are present in the cytoplasm of endothelial cells (black arrowheads) and overlapping endothelial cells are separated by a more electron lucent layer (white arrows). (**k**) $CD31^+$ staining of endothelial cells clearly shows enlarged dilated capillaries 3 days after ouabain exposure. $CD31^+$ capillaries are identified by the white arrows. Scale bars, 2 µm in **b–d**, and **g**; 6 µm in **e**; 5 µm in **f**; 1.5 µm in **h**; **i** and **j**; 40 µm in **l**; 2.5 µm in an enlarged image of the boxed area in **f;** 800 nm in an enlarged image of the boxed area in **g;** 60 µm in **l** (Applicable to **k**).

and Sox2 was performed. $GFP^+/Sox2^+$ cells were seen infrequently in the injured ANs (**Figure 4g**) but were never observed in control non–ouabain-exposed ears (data not shown). When dual immunostaining was conducted for the spiral ganglion neuronal marker neurofilament 200 (NF200),[17] no $NF200^+$ SGNs were positive for GFP (data not shown).

Enhanced homing and tissue engraftment of human HSCs in the injured AN of NSG mice

Our findings of enhanced homing and tissue engraftment of mouse hematopoietic cells in the ouabain-exposed AN led us to investigate if human hematopoietic cells can likewise engraft and differentiate in the injured adult AN. Mouse xenograft models based on severely immune-incompetent mice are widely used to investigate the biology of human HSCs *in vivo*.[23] We employed a human-murine xenograft model in our laboratory using NSG mice as human cell recipients (**Figure 5a**). Flow cytometric analysis of peripheral blood samples revealed positive human cell engraftment in 8 of 11 transplanted mice at 2–6 months after injection of human $CD34^+$ cord blood cells. The peripheral blood engraftment levels in these eight mice were 46, 45, 24, 20, 20, 12, 12, and 8% (**Supplementary Figure S1**). An analysis of bone marrow samples of these mice revealed the percentages of the B-cell ($CD19^+$), T-cell ($CD3^+$), and granulocyte/macrophage ($CD11b^+$)

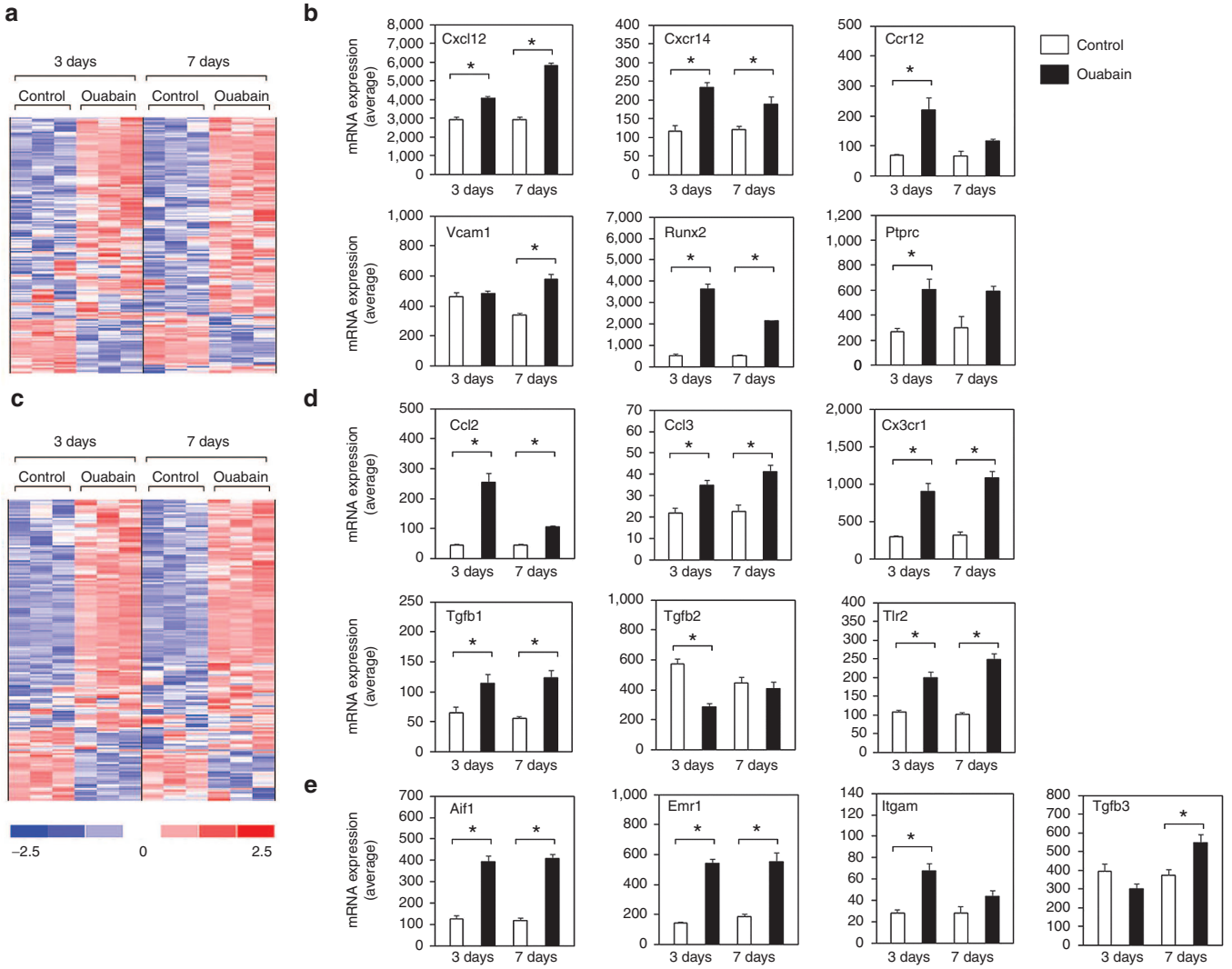

Figure 3 Ouabain-induced upregulation of genes associated with HSC homing and macrophage differentiation and activation. (**a**) Microarray data show that 180 genes associated with HSC differentiation and homing were differentially expressed in response to ouabain, *i.e.*, genes scored $P < 0.05$ (Student's *t*-test, unpaired, two-tailed, not assuming equal variance) in either 3 or 7 day ouabain treatment samples in comparison to the matched-time contralateral controls. False discovery rate for this comparison approximated 10% based on iterative comparisons involving randomized sample groupings. (**b**) Expression values are shown for representative HSC homing and differentiation genes upregulated after ouabain injury. (**c**) 164 genes associated with macrophage/microglia activity were differentially expressed at either 3 or 7 days after ouabain treatment using the comparison approach described above. False discovery rates for this comparison approximated 7%. (**d**) Expression values of several representative genes associated with macrophage activation and differentiation were increased in the injured AN. (**e**) Expression values are shown for several macrophage marker genes that also were increased in the injured AN. Colorimetric scaling (Z-standardization) for heatmaps is shown at bottom left.

lineages among human CD45⁺ cells ranged from 12 to 38%, from 69 to 71%, and from 53 to 71%, respectively. Data from one of the transplanted NSG mice is shown in **Figure 5b**, where the percentages of the B-cell, T-cell, and granulocyte/macrophage lineages among human CD45⁺ cells in bone marrow at six months after human cell injection were 25, 0.9, and 18%, respectively.

To determine if cochlear injury affected the levels of HSC homing and tissue engraftment in the AN, NSG mice transplanted with human CD34⁺ cells were subjected to cochlear injury with ouabain. As shown in **Figure 5c**, ouabain exposure caused a dramatic loss of SGNs by 7 days based on the reduced number of cells immunoreactive for the SGN cellular marker TuJ1 (neuron specific beta-III tubulin).[50,51] Tissue engraftment of the human cells was evaluated in cochlear sections of ouabain-exposed recipient mice through immunohistochemical detection of two human cell-specific markers, anti-human nuclear antibody (AHA; **Figure 5d–i**) or anti-human mitochondria antibody (AHMA; data not shown). Staining for these markers demonstrated that human cells engrafted in several areas of the inner ear, including the spiral ligament of the cochlear lateral wall (**Figure 5e** and **Figure 6a,c**), the AN in the osseous spiral lamina (**Figure 5f** and **Figure 7**), and Rosenthal's canal in all three turns of the cochlear duct (**Figure 5g–i** and **Figure 6b,d**). A small number of human-derived cells were also seen in the vestibular ganglion and stroma underlying the sensory epithelium of the vestibular organ (not shown). As shown in **Figure 5k**, quantitative analysis of immunohistochemical

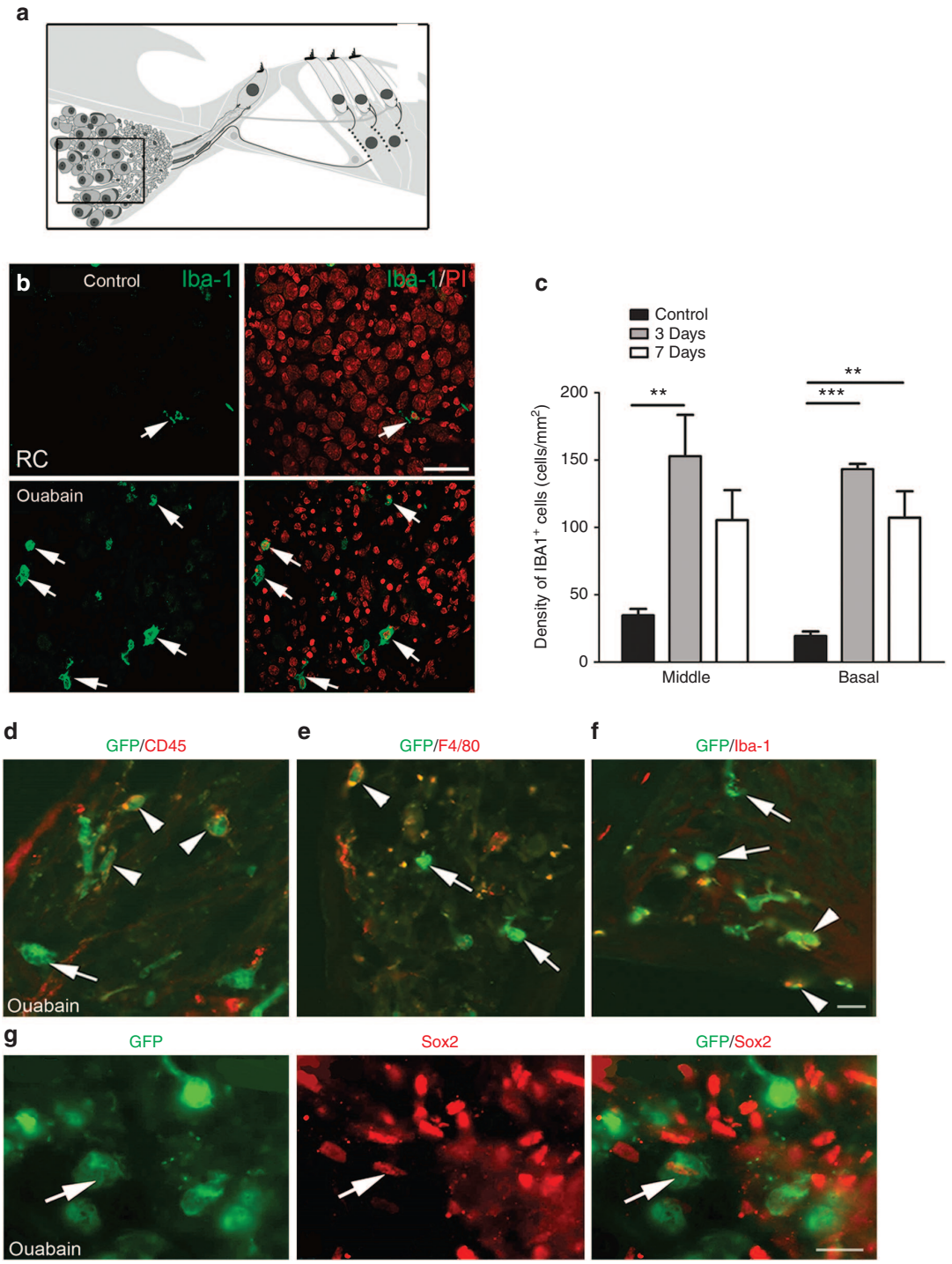

Figure 4 Infiltration of macrophages and bone marrow-derived macrophages and nonmacrophage cells into the ouabain-treated AN. (**a**) Schematic of peripheral auditory nerve. The macrophages were quantified in Rosenthal's canal (boxed area). (**b**) Staining for Iba-1$^+$ macrophages in the spiral ganglion (white arrows) was markedly increased 3 days after ouabain exposure. (**c**) Quantitative analysis of Iba-1$^+$ cell density revealed a significant increase in Iba-1$^+$ cell numbers after ouabain exposure in both the middle and basal portions of the cochlea (**$P < 0.01$; ***$P < 0.001$; Data represent mean ± SEM; $n = 3$–5 mice per condition; the values of p and t for the comparisons between control with 3 days treatment and control with 7 days treatment in the middle turn were 0.0036 and 4.29, and 0.0067 and 4.050, respectively; the values of P and t for the comparisons between control with 3 days treatment and control with 7 days treatment in the basal turn were 0.0001 and 23.51, and 0.0117 and 4.403, respectively; unpaired t-test). (**d**–**f**) Both GFP$^+$ macrophages (white arrowheads) and GFP$^+$ nonmacrophages (white arrows) were present in injured ANs. Cochlear tissues were stained with antibodies against CD45, F4/80, or Iba-1. (**g**) A GFP$^+$ cell (white arrow) stains positively for the transcriptional factor Sox2, a widely used neural progenitor cell marker. Scale bars, 30 μm in **b**; 10 μm in **f** and **g**.

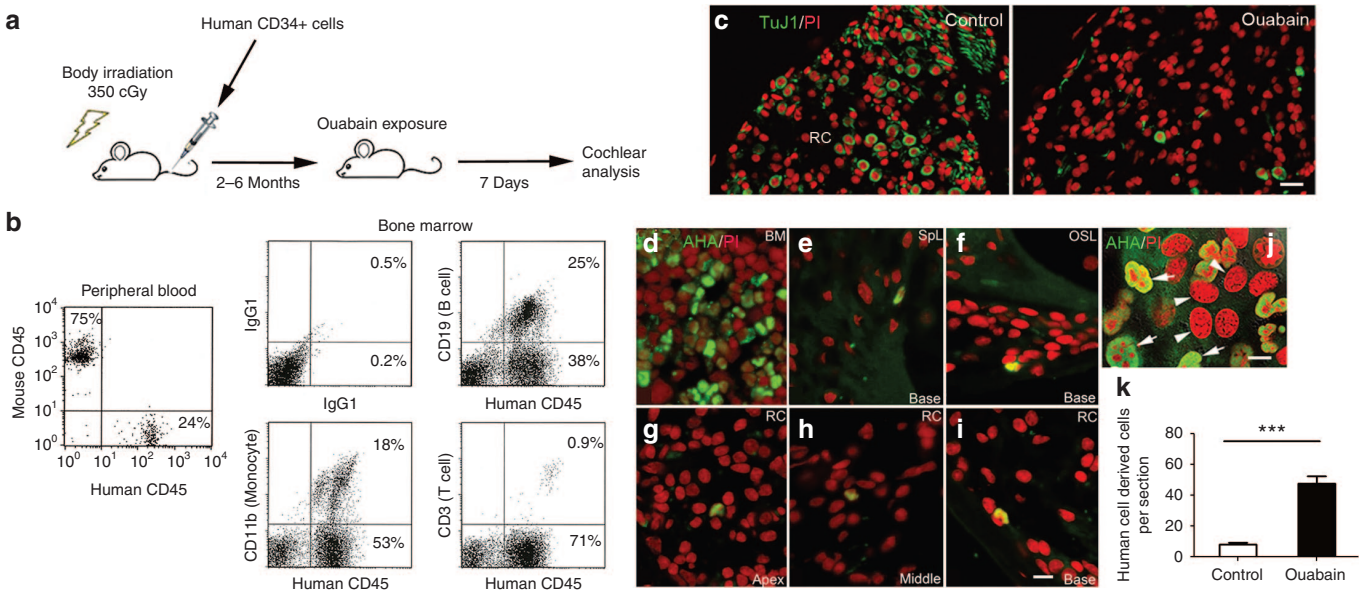

Figure 5 Enhanced tissue engraftment of human CD34⁺ cord blood cells in ouabain-treated ANs in a humanized transplantation model. (**a**) Experimental approach using humanized mice and AN injury. (**b**) Multi-lineage hematopoietic reconsititution from CD34⁺ cord blood cells. The data shows flow cytometric analysis of nucleated peripheral blood and bone marrow cells obtained from a representative NSG mouse six months after injection with 2.0×10^5 CD34⁺ human cord blood cells. Reconstitution by human CD45⁺ cells in mouse peripheral blood was 24%. Reconstitution in bone marrow by human CD19⁺ (B cells), CD11b⁺ (monocytes) and CD3⁺ (T cells) was 25, 18, and 0.9%, respectively. (**c**) Ouabain destroys almost all SGNs (Tuj1⁺) in the cochlea of a representative transplanted NSG mouse. (**d**) Abundant human cells identified by immunostaining with anti-human antigen (AHA) are present in the BM. (**e–i**) Human cells derived from cord blood HSCs (AHA⁺ cells) are present in several locations in the cochlea of a mouse 5 months after transplantation. The images were obtained 7 days after exposure of the cochlea to ouabain and include the spiral ligament (SpL; **e**), the osseous spiral lamina (OSL; **f**) and Rosenthal's canal (RC; **g–i**) from the apical, middle, and basal turns. (**j**) Human cells (human lung cancer cell line A549) were cocultured with mouse cells (mouse auditory neuroblast cell line N33). Human cell nuclei (white arrows) are stained green with AHA, whereas nuclei of mouse cells remain unlabeled (white arrowheads). (**k**) The tissue engraftment of human HSC-derived cells increased significantly in the AN of ears exposed to ouabain. Data was obtained from the left (control) and right (ouabain exposed) ears of NSG mice (***$P < 0.001$; data represent mean ± SEM; $n = 5$ mice per group; $P = 0.00005$; $t = 18.14$; unpaired t-test). Scale bars = 25 µm in **c**; 10 µm in **i** (applicable to **d–h**); 7 µm in **j**.

data demonstrated that the number of human cells was significantly increased in ouabain-treated cochleas as compared to control samples ($P < 0.001$, Student's t-test,unpaired).

Differentiation of human hematopoietic cells in the injured mouse AN

To further characterize the phenotype of engrafted human cells, dual immunolabeling procedures were performed on cochlear sections using AHA and antibodies specific for different cochlear cell populations including those recognizing macrophages (Iba1), glial cells (Sox2 and Sox10), neurons (TuJ1), and endothelial cells (CD31). First, we employed dual immunostaining with the AHA antibody and rabbit anti-Iba-1 antibody which recognizes human and rodent Iba-1 protein to examine the potential of human hematopoietic cells to differentiate into macrophage cells. The human cell-derived populations of macrophages (AHA⁺/Iba-1⁺) and nonmacrophages (AHA⁺/Iba-1⁻ cells) were quantified throughout control and ouabain-injured cochleae of transplanted mice. As shown in **Figure 6a–d**, human CD34⁺ cells can give rise to both Iba-1⁺ macrophages and non-Iba-1⁺ cells. Over 45% of the engrafted human-derived cells failed to stain for the macrophage marker Iba-1 in the injured AN, whereas less than 10% of engrafted human-dervied cells were Iba-1 negative in control ears (**Figure 6e**; $P < 0.001$; Student's t-test,unpaired), suggesting that cochlear injury enhances the differentiation of human non-macrophage cell types in the AN. We then examined whether engrafted cells in the AN differentiated into endothelial or glial cells. Approximately 20% of the AHA⁺ cells were located in the cochlear nerve tissue, but none of them stained positively with an antibody specific for the human endothelial marker CD31. However, a few of these cells were positive for Sox10 (**Figure 7**), a neural crest-derived cell and glial cell marker that is predominantly expressed in proliferating and undifferentiated neural precursors during neurogenesis.

F4/80 (Emr1/Adgre1) is a commonly used marker for the identification of mouse microglial cells and tissue macrophages in the mouse inner ear.[49,52] Interestingly, the human ortholog of F4/80 (EMR1/Adgre1) is not present on human mononuclear phagocytic cells including macrophages, monocytes, and myeloid dendritic cells.[53] This distinction allows us to detect mouse macrophages specifically in animals transplanted with human cells. Thus, we could detemine if mouse macrophages (F4/80⁺) phagocytize degenerative human derived cells in the injured AN of transplanted mice by dual-labeling for AHA and mouse F4/80 and then examining apoptotic profiles in AHA⁺ nuclei. As shown in **Figure 8**, some AHA⁺ nuclei were seen to be accompanied by F4/80⁺ cytoplasmic processes (**Figure 8a**) on sections from ouabain-treated ears of NSG mice, although most F4/80⁺ cells did not show colocalization with AHA⁺ cells or engulfment of AHA⁺ nuclei (**Figure 8e**). Similarly, AHA⁺ nuclei were often not colocalized with F4/80⁺ cytoplasmic processes (**Figure 8b–d** and **Figure 8f**).

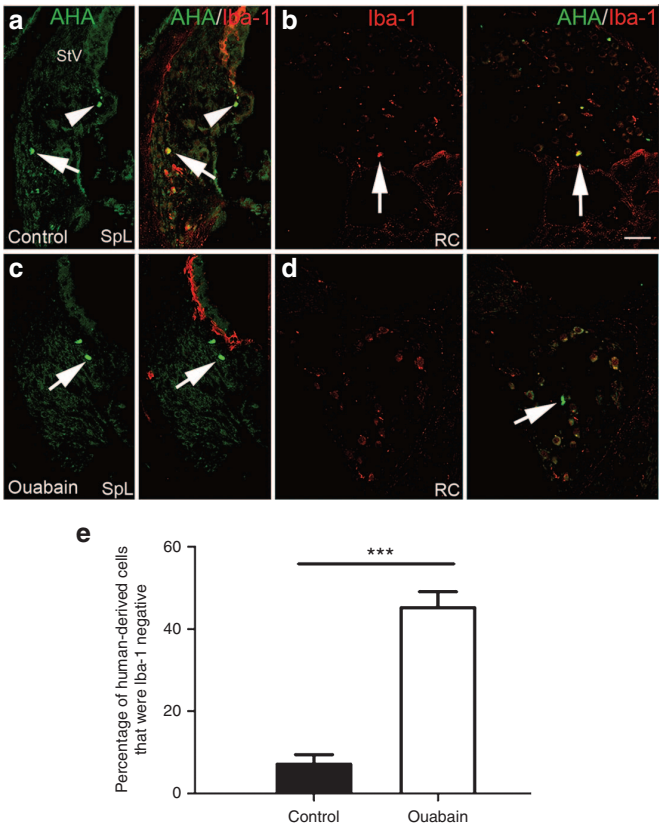

Figure 6 Human HSCs differentiated into both Iba-1⁺ macrophages and Iba-1⁻ cells in the injured AN. (**a–d**) Images were taken from cochleas of NSG mice injected with CD34⁺ human cord blood cells. Ouabain was applied to the right ear of each mouse and cochlear tissues from control (left) and injured ears were examined 7 days later. (**a**,**b**) Human-derived macrophage cells were stained positively (arrows) and negatively (arrowheads) in the SpL and RC of a control ear. (**c**,**d**) Human-derived cells in the SpL and RC failed to stain with Iba-1 antibody (arrows) in an ouabain-treated ear. (**e**) Cell count analysis indicated AN injury increased the percentage of human cell-derived Iba-1⁻ non-macrophage cells among the total engrafted human-derived cell population in recipient mouse ears (***$P < 0.001$; $n = 5$ mice per group; $P = 1.76294$ E–08; $t = 75.57$; unpaired t-test). Scale bar, 45 µm in **d** (applied to **a–c**).

Examination of 75 mid-modiolar sections randomly selected from control ears (15 sections per ear; 5 ears) and ouabain-treated ears (15 sections per ear; 5 ears) found 330 and 990 AHA⁺ nuclei, respectively, that were not in apparent association with F4/80⁺ cytoplasmic processes; there were 174 and 878 AHA⁺ nuclei, respectively, that were in apparent association with F4/80⁺ cytoplasmic processes. For the AHA⁺ nuclei in apparent association with F4/80⁺ cytoplasmic processes (**Figure 8a**), none of the nuclei displayed an apoptotic nuclear profile, which is recognized by the the appearance of chromatin condensation and apoptotic bodies.

The perineural sheath around the peripheral nerves plays an important role in maintaining the integrity of the nerve microenvironment by creating a physical barrier that limits entry of toxic agents into nerve bundles.[54] **Figure 8f** shows that a cluster of perineural cells in the injured AN were AHA⁺, but appeared without the presentation of F4/80⁺ cytoplamic processes. Together, these results suggest that host macrophage phagocytosis of degenerative AHA⁺ human cells, if it occurs at all, is a very rare event in the injured auditory nerves of the recipient NSG mice.

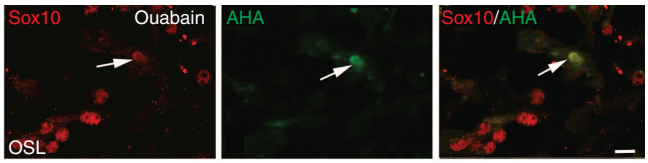

Figure 7 Human HSCs differentiate into Sox10⁺ glial-like cells. Images were obtained from the ouabain-exposed ear of a transplanted NSG mouse. Ouabain was applied to the right ear of the transplanted mouse and cochlear tissues from control (left) and injured ear were examined 7 days later. Immunostaining for Sox10 (red) and AHA (green) in the AN of a human CD34⁺ cell transplanted mouse. Arrow points to the same cell in all three images. Scale bar = 7 µm.

DISCUSSION

In this study, we found that cochlear injury enhances tissue engraftment and differentiation of both mouse and human hematopoietic cells in the adult AN. Injury-induced disturbances of the microvasculature and upregulation of genes associated with HSC homing provide a critical local microenvironment beneficial to homing and distribution of hematopoietic cells in the AN and other cochlear regions. Examples of genes associated with HSC homing upregulated by AN injury included Cxcl12 (SDF-1), Cxcr4, Ccr2, Vcam, and Runx2. At the same time, the expression of several molecules known as hematopoietic and macrophage/microglial cell makers were also found to increase in the injured ANs. These molecules included Ptprc and the macrophages/microglial cell makers Aif1, Emr1, and Itgam.

The upregulated expression of Cxcl12 identified in this study by gene array analysis confirms data from our previous study showing that Cxcl12 protein expression was increased in the injured AN using the same ouabain exposure mouse model.[55] Homing and engraftment of circulating stem/progenitor cells into injured tissues and organs is largely controlled by interactions between the chemokine Cxcl12 and Cxcr4.[56,57] Upregulation of Cxcl12 expression has been shown to correspond to an increase in migration and homing of circulating Cxcr4⁺ stem/progenitor cells into ischemic tissues.[58] It is also well-established that Cxcl12 is highly conserved among different species with human and murine Cxcl12 differing by only one amino acid.[59] The interactions between Cxcl12 and Cxcr4 are essential to the migration, homing, and tissue engraftment of human stem cells in immunodeficient mice.[57,60] A previous study using the human-murine xenograft model demonstrated that cytokines produced by liver injuries promoted both increased Cxcr4 expression and the recruitment of human HSCs in the liver of NOD/SCID mice.[61] Thus, it is likely that the homing and tissue engraftment of human CD34⁺ cells into the injured adult AN in the humanized mouse model is based on the direct interaction between human chemokine receptor Cxcr4 and mouse Cxcl12.

Another important finding here was that acute nerve injury significantly increased the number of hematopoietic cell-derived macrophages in the adult AN. Cochlear macrophages are an essential part of the resident mononuclear phagocyte population in the peripheral auditory system.[62,63] Recruitment of CD45⁺ macrophages has been documented in several locations of the adult cochlea following acoustic or ototoxic injury.[33,49,64] In the central nervous system, highly motile microglia constantly monitor the

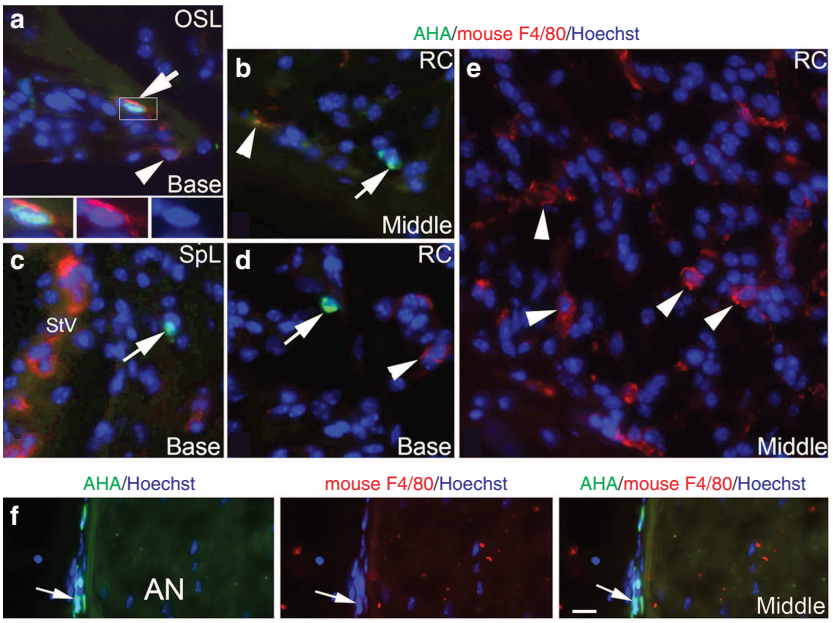

Figure 8 No engulfment of degenerative CD34⁺ human cells by mouse F4/80⁺ macrophages seen in the injured AN. (**a–e**) Images were taken from cochleae of NSG mice injected with CD34⁺ human cord blood cells. Ouabain was applied to the right ear of each mouse and cochlear tissues from control (left) and injured ears were examined 7 days later. (**a**) An AHA⁺ cell (green) in the osseous spiral lamina (OSL) was partially engulfed by cytoplasmic processes stained positively for the mouse macrophage-specific marker F4/80 (arrow). Three images at the bottom represent enlarged images of the boxed area showing the nucleus (blue) of an AHA⁺ cell (green) surrounded by a mouse F4/80⁺ macrophage (Red). (**b–d**) Several AHA⁺ cells (arrows) located in Rosenthal's canal (RC; **b,d**) and the spiral ligament (SpL; **c**) were not seen in association with F4/80 positive macrophages. (**e**) Numerous F4/80⁺ macrophages are present in RC in the middle turn. (**f**) A cluster of AHA⁺ cells (green) were present along the perineurium of the injured AN. These human derived cells (arrows) did not co-label with F4/80 or be engulfed by mouse F4/80⁺ macrophages (red). Nuclei were counterstained with Hoechst (blue). Scale bar = 15 μm in **f** (applied to **a–d**).

local microenvironment under both normal and pathological conditions and are involved in regulating several important cellular events including cell death, survival, proliferation and differentiation.[27] Although early studies investing the roles of microglial cells/macrophages in nerve injury/repair focused mainly on their role in cleaning degenerative cellular debris and other apoptotic cells after injury,[65] it is obvious that microglial cells/macrophages also play a critical role in remodeling the microenvironment for the enhancement of the nerve tissue repair and function recovery.[66] Blocking microglial activation through either pharmacologic or genetic approaches exacerbates nerve lesions and impairs function recovery.[67,68] A recent study revealed that macrophage recruitment promotes the survival of SGNs after hair cell death through fractalkine signaling.[11]

In earlier work,[2] we demonstrated a significant increase in proliferative glial cells of the AN within Rosenthal's canal and the osseous spiral lamina 3–7 days after ouabain exposure. As demonstrated here, enhanced tissue engraftment of the hematopoietic cells and macrophage infiltration was seen in these same areas. The data suggests that recruited macrophages, which are derived from hematopoietic cells, are involved not only in removing degenerative SGNs, but also in regulating proliferation of glial cells and promoting nerve tissue repair in the injured AN. It is possible that the low rate of glial turnover seen in the adult cochlea under normal conditions is mediated by mitosis of resident glial cells or their progenitor cells whereas the enhanced proliferation of glial cells after injury may be regulated by newly recruited bone marrow-derived or circulating stem/progenitor cells.

Our results also demonstrate that a subset of the differentiated cells lack macrophage markers in the injured ANs of both human cord blood (CB) and mouse HSC transplantation models. This finding suggests that hematopoietic cells may also participate directly in the replacement of non-neuronal cells in adult cochlear nerve tissues. Previous studies support the concept that tissue injury enhances the homing, tissue engraftment and differentiation of circulating stem/progenitor cells.[69–71] Harris *et al.*[72] documented that injury to the retinal pigment epithelium (RPE) significantly increases the recruitment of bone marrow-derived cells into the RPE layer. A portion of the engrafted bone marrow-derived cells adopted RPE cell morphology, expressed RPE cell markers and integrated into RPE without cell fusion. A population of multipotent progenitor cells (MPCs), which express the transcription factor Sox2 along with Nanog, Oct3/4, cMyc, and Klf4 has been identified in human peripheral blood.[73] Under enriched culture conditions, these MPCs were capable of differentiating into multiple cell types including neurons, glia, endothelial cells, osteoblasts, hepatocytes, and cardiomyocytes. In a previous study using transplantation of a clonal population of HSCs derived from a single HSC, we found that nonsensory cochlear cells, such as fibrocytes in the spiral ligament of the adult mouse, are continually derived from bone marrow HSCs.[17] The establishment here of a humanized model using NSG mice allowed us to investigate tissue engraftment of human CD34⁺ hematopoietic cells in the adult AN. The high population of human CD45⁺ cells in recipient mice enabled us to identify and characterize the differentiation of human CD34⁺ cells in the adult mouse AN and other cochlear

regions. Using this model, we demonstrated that human CD34$^+$ cord blood cells are capable of generating perineural and glial-like cells in the inner ears of transplanted mice although this occurs infrequently. These results suggest that HSCs are an important moderator for the homeostasis of normal adult nerve tissues in addition to their role in neural plasticity and nerve tissue repair and regeneration after injury and in other pathological conditions.

The results presented here showed, for the first time, that acute nerve injury significantly increases tissue engraftment and differentiation of human CD34$^+$ cells in the cochlea of recipient mice. Analysis of cochlear sections immunostained with specific cellular markers indicated that human cells are capable of differentiating into both macrophages and other cell types. These findings suggest that transplantation of human CB CD34$^+$ cells may be a useful approach to manipulate the cochlear microenvironment to enhance repair/regeneration of degenerative AN.

In summary, our data demonstrate that transplanted hematopoietic cells from both mice and humans can engraft and differentiate into macrophages and other cell types in the adult AN, particularly after SGN loss. Structural changes in the microvasculature and upregulation of genes associated with HSC homing and differentiation in the injured AN provide a constructive microenvironment for hematopoietic cell tissue engraftment and differentiation in the adult AN.

MATERIALS AND METHODS

Animals. Transgenic mice (C57BL/6-Ly5.2) with enhanced GFP were kindly provided by Dr. Masaru Okabe of Osaka University, Osaka, Japan.[74] Adult CBA/CaJ, C57BL/6-Ly5.1 and NSG mice were purchased from Jackson Laboratories (Bar Harbor, ME).[25] All four strains of mice were maintained and bred in the Animal Research Facility at the MUSC or Veterans Affairs Medical Center. All aspects of the animal research were conducted in accordance with the guidelines by the Institutional Animal Care and Use Committee of the MUSC and Department of Veterans Affairs Medical Center. Experimental procedures were reviewed and approved by the Institutional Animal Care and Use Committees (IACUC) at MUSC under protocol number AR2845 (H.L.) and the IACUC of the Ralph H. Johnson VAMC under protocol number AR450 (A.C.L.). Prior to experimental processes, adult mice were examined for signs of external ear canal and middle ear obstruction. Mice with any symptoms of middle ear infection were excluded from the study. Both male and female mice were randomly selected in the experimental groups.

Cell preparation and transplantation. Ten- to 12-week-old enhanced GFP transgenic mice were used as BM donors for mouse-mouse transplantation studies. The mice were euthanized by CO_2 inhalation and BM cells were flushed from tibiae and femurs, pooled together and washed with Ca^{2+} and Mg^{2+} free phosphate-buffered saline (pH 7.4) (Life Technologies, Grand Island, NY) containing 0.1% bovine serum albumin (Sigma-Aldrich, St. Louis, MO). GFP$^+$ mononuclear cells cells with a density of 1.0875 ± 0.0019 g/ml were collected by gradient separation using Lympholyte M (Ontario, Canada). Three-month-old C57BL/6-Ly5.1 mice were used as recipients. Recipient mice were prepared with a single 950-cGy dose of total body irradiation using a 4×10^6 V linear accelerator. For BM cell transplantation, 1×10^6 un-manipulated BM cells obtained from GFP mice were injected into the tail veins of adult irradiated Ly5.1 mice. The dosage and concentration of the un-manipulated BM cells used for the transplantation was determined in previous studies.[17,28,34]

For human-mouse CB cell transplantation, human CD34$^+$ CB cells were purchased from StemCell Technologies Inc (Catalog number: CB007F-S; CB090918A; Vancouver, BC). Cryo-preserved cells were thawed in cold α minimum essential medium (GIBCO, Invitrogen, Carlsbad, CA) containing 20% fetal bovine serum (Atlanta Biologicals, Norcross, GA) and washed with phosphate-buffered saline (Invitrogen). Recipient adult mice were exposed to a single dose of radiation (350cGy) in a period of 10–12 minutes and 2.0×10^5 human CD34$^+$ cord blood cells were injected into the tail vein. The CD34$^+$ cell injection dosage was determined based on previous studies of human CD34$^+$ cell transplantation with several receipt mouse models.[75–77] Irradiated animals were housed in sterile cages, fed sterile chow and provided with drinking water supplemented with neomycin (1 mg/ml) to prevent infections while mice were immunosuppressed (up to 2 weeks post-transplant).

Flow cytometric analysis of hematopoietic engraftment. For mouse-mouse bone marrow transplantation, flow cytometric analyses of hematopoietic engraftment were performed on recipient mice prior to euthanasia. Peripheral blood was obtained from the retro-orbital plexus of the recipient mice using heparin-coated micropipettes (Drummond Scientific, Broomall, PA). Red blood cells were lysed with 0.15 M NH_4Cl and the cells were stained with PE-conjugated anti-Ly5.1. The percentage of chimerism was calculated as (% GFP$^+$ cells) × 100/ (% GFP$^+$ /Ly5.1$^+$ cells). For the analysis of hematopoietic engraftment on human-mouse transplantation models, blood was obtained from the tail vein of recipient mice 2–3 months after transplantation. Red blood cells were lysed with PharM Lyse (BD Pharmingen, San Diego, CA). Human cells were detected by staining with fluorescein (FITC)-conjugated anti-human CD45 antibody (BD Pharmingen). Recipient mice with a high percentage of human CD45$^+$ cells were selected for the AN injury experiments and euthanized for analyses at specific time windows. BM cells were flushed from the femurs and tibiae of recipient mice using a U-100 Insulin Syringe with 28-gauge needles (Becton-Dickinson and Company, San Jose, CA) and washed with phosphate-buffered saline containing 0.1% bovine serum albumin (Sigma-Aldrich). The samples were processed into a single-cell suspension via frequent passage through a 22G needle (Becton-Dickinson and Company) and filtered with a 40 μm nylon mesh cell strainer (Becton-Dickinson and Company). Mononuclear cells with densities <1.0875 ± 0.0019 g/ml were collected by gradient separation using Lympholyte M. Lineage expression of the engrafted cells was analyzed with PE-conjugated anti-human CD11b (BD Pharmingen), PE-conjugated anti-human CD19 (BD Pharmingen), and PE-conjugated anti-human CD3 (BD Pharmingen) along with FITC-conjugated anti-human CD45. The samples were resuspended in phosphate-buffered saline with PI 1 μg/ml and analyzed with a FACSCalibur (Becton-Dickinson and Company).

Ouabain exposure and microsurgical procedures. Surgical procedures were modified from previous studies.[39] The timing of surgical procedures performed using the transplanted mouse models are described in **Figures 1** and **5**. Briefly, adult CBA/CaJ and recipient mice were anesthetized with xylazine (10 mg/kg, i.p.) and ketamine (100 mg/kg, i.p.). Survival surgery was performed under sterile conditions. Buprenorphine (0.1 mg/kg, i.p.) was administered 30 minutes before the surgery to minimize any surgical discomfort. Sterile procedures were used to open the bulla and deliver ~10 μl of 3 mmol/l ouabain (Sigma-Aldrich, O3152) solution to the round window niche. The total time of ouabain exposure was approximately 60 minutes; every 10 minutes the ouabain solution was wicked away with filter paper wicks and a fresh solution was applied. The right ear was the operative ear while the left ear served as a control. Following treatment with ouabain, mice were allowed to recover for 3 or 7 days.

Tissue collection, and morphological and immunohistochemical analysis. Cochleae of the recipient mice were fixed with a 4% paraformaldehyde solution for 1–2 hours at room temperature (RT), decalcified with 0.12 M ethylenediamine tetraacetic acid at RT with stirring followed by dehydration in a 30% sucrose solution. The tissues were then embedded in Tissue-Tek OCT compound, frozen, and sectioned at 10 μm thickness. Sections were immersed in blocking solution for 20 minutes and then incubated overnight at 4 °C with a primary antibody diluted in

0.2% bovine serum albumin. The primary antibodies used in this study are listed in **Supplementary Table S3**. Secondary antibodies were biotinylated and binding was detected by labeling with FITC-conjugated avidin D or Texas red-conjugated avidin D (Vector Labs, Burlingame, CA). Nuclei were counterstained with propidium iodide (PI), bis-Benzimide, or 4′,6-diamidino-2-phenylindole. Sections were examined on a Zeiss LSM5 Pascal confocal microscope or Olympus Fluoview FV1000 confocal microscope. FITC and Texas red (or PI) signals were detected by excitation with the 488 and 543 nm lines, respectively. Images were scanned at scales of 0.29 μm (x) × 0.29 μm (y) and a stack size of 146.2 μm (x) × 146.2 μm (y) with a Plan-Apochromat 63×/1.4 Oil DIC objective (Carl Zeiss, Germany). Captured images were processed using Zeiss LSM Image Browser Version 3.2.0.70 (Carl Zeiss, Jena, Germany) and Adobe Photoshop CS.

Transmission electron microscopy. Anesthetized animals were perfused via cardiac catheter with 10 ml of normal saline containing 0.1% sodium nitrite followed by 15 ml of a mixture of 4% paraformaldehyde and 2% glutaraldehyde in 0.1 M phosphate buffer, pH 7.4. After removing the stapes and opening the oval and round windows, 0.5 ml of the same fixative described above was perfused gently into the scala vestibuli through the oval window. Inner ears were dissected free and immersed in fixative overnight at 4 °C. Decalcification was completed by immersion in 40 ml of 120 mmol/l solution of ethylenediamine tetraacetic acid, pH 7.0, with gentle stirring at room temperature for 2–3 days, with daily changes of the ethylenediamine tetraacetic acid solution. Cochlear tissues were post-fixed with 1% osmium tetroxide-1.5% ferrocyanide for 2 hours in the dark, then dehydrated and embedded in Epon LX 112 resin. Semi-thin sections approximately 1 micrometer thick, were cut and stained with toluidine blue. Ultrathin sections (70 nm thick) were stained with uranyl acetate and lead citrate and examined by electron microscopy.

Bioinformatic analysis of microarray data obtained from ouabain-treated mouse AN. Microarray analysis of ouabain-treated mouse ANs has been previously described[39]; normalized expression data associated with this study is deposited in NCBI Gene Expression Omnibus under the series accession GSE59417. HSC homing and differentiation genes for analysis were designated based on Gene Ontology (GO) Database annotation terms relating to HSC proliferation (GO:0071425), differentiation (GO:0002244), and migration (GO:2000471; GO:0035701) and other published associations. Macrophage activation and marker genes were designated based on GO annotations relating to macrophage activation (GO:0042116), mediation of immune response (GO:0002700), and chemotaxis (GO:0048246) and other published associations. For genes in each group, differential expression was tested by Student's *t*-test, unpaired, two-tailed, not assuming equal variance, for ouabain treatment at either 3 or 7 days after ouabain exposure in comparison to the matched-time contralateral controls ($n = 3$ for all sample types). Significance was assigned for genes with $P < 0.05$ at either time point. Comparison outcomes were as follows: (i) HSC homing and differentiation genes, 180 of 389 genes significantly different, estimated false discovery rate of 10.6%; (ii) macrophage activation and marker genes, 164 of 346 genes significantly different, estimated false discovery rate of 7.4%. False discovery rates were estimated by iterative permuted comparisons involving randomized sample groupings.

Data analysis. Cell counts for the Iba-1$^+$ and GFP$^+$ cells in mouse-mouse transplantation experiments were performed on 5–6 mid-modiolar sections per ear taken at least 25-μm apart. Cell counts for the AHA$^+$, AHA$^+$ /Iba-1$^+$, AHA$^+$/mouse F4/80$^+$, AHA$^+$/mouse F4/80$^-$, and AHA$^+$ /Iba-1$^+$ on human-mouse transplantation experiments were conducted on 15–20 mid-modiolar sections per ear taken at least 10-μm apart. Unless otherwise specified, all data in the figures are presented as mean ± standard error of the mean. Data for the density of Iba-1$^+$, GFP$^+$, and AHA$^+$ cells, and comparisons of gene expression levels in gene array assays were analyzed by two tailed, unpaired Student's *t*-test. A value of $P < 0.05$ was considered to be statistically significant.

SUPPLEMENTARY MATERIAL

Figure S1. Flow cytometry of nucleated blood cells demonstrates robust engraftment (from 8–45%) in peripheral blood from eight recipient NSG mice 2–6 months after injection of human CD34$^+$ cord blood cells.

Table S1. Genes associated with HSC homing and differentiation that were differentially expressed in the AN following ouabain exposure.

Table S2. Genes associated with macrophage/microglia activity that were differentially expressed in the AN following ouabain exposure.

Table S3. Antibody information.

ACKNOWLEDGMENTS

This work has been supported by National Institutes of Health Grants R01DC012058 (H.L.), and P50DC00422 (H.L., B.A.S.). J.L.B. and microarray data analyses were additionally supported through GM103342, GM103499, and MUSC's Office of the Vice President for Research. We thank Makio Ogawa for preliminary planning of this project, Meenal Mehrotra for her help with the hematopoietic cell transplantation, Juhong Zhu for cochlear tissue preparations, and Mary Bridges, Clarisse Panganiban, and Linda McCarson for their critical comments on the manuscript. The authors declare no competing financial interests.

AUTHOR CONTRIBUTIONS

H.L. designed the research; H.L., E.N., Y.X., and J.B. performed the research; H.L., B.S., Y.X., L.B., K.N., K.A., and A.L. analyzed the data; H.L., J.B., and B.S. wrote the paper.

REFERENCES

1. Roberson, DW and Rubel, EW (1994). Cell division in the gerbil cochlea after acoustic trauma. *Am J Otol* **15**: 28–34.
2. Lang, H, Schulte, BA and Schmiedt, RA (2003). Effects of chronic furosemide treatment and age on cell division in the adult gerbil inner ear. *J Assoc Res Otolaryngol* **4**: 164–175.
3. Lang, H, Jyothi, V, Smythe, NM, Dubno, JR, Schulte, BA and Schmiedt, RA (2010). Chronic reduction of endocochlear potential reduces auditory nerve activity: further confirmation of an animal model of metabolic presbyacusis. *J Assoc Res Otolaryngol* **11**: 419–434.
4. Schulte, BA and Schmiedt, RA (1992). Lateral wall Na,K-ATPase and endocochlear potentials decline with age in quiet-reared gerbils. *Hear Res* **61**: 35–46.
5. Spicer, SS, Gratton, MA and Schulte, BA (1997). Expression patterns of ion transport enzymes in spiral ligament fibrocytes change in relation to strial atrophy in the aged gerbil cochlea. *Hear Res* **111**: 93–102.
6. Sakaguchi, N, Crouch, JJ, Lytle, C and Schulte, BA (1998). Na-K-Cl cotransporter expression in the developing and senescent gerbil cochlea. *Hear Res* **118**: 114–122.
7. Hirose, K and Liberman, MC (2003). Lateral wall histopathology and endocochlear potential in the noise-damaged mouse cochlea. *J Assoc Res Otolaryngol* **4**: 339–352.
8. Sautter, NB, Shick, EH, Ransohoff, RM, Charo, IF and Hirose, K (2006). CC chemokine receptor 2 is protective against noise-induced hair cell death: studies in CX3CR1(+/GFP) mice. *J Assoc Res Otolaryngol* **7**: 361–372.
9. Sato, E, Shick, HE, Ransohoff, RM and Hirose, K (2008). Repopulation of cochlear macrophages in murine hematopoietic progenitor cell chimeras: the role of CX3CR1. *J Comp Neurol* **506**: 930–942.
10. Sato, E, Shick, HE, Ransohoff, RM and Hirose, K (2010). Expression of fractalkine receptor CX3CR1 on cochlear macrophages influences survival of hair cells following ototoxic injury. *J Assoc Res Otolaryngol* **11**: 223–234.
11. Kaur, T, Zamani, D, Tong, L, Rubel, EW, Ohlemiller, KK, Hirose, K *et al.* (2015). Fractalkine signaling regulates macrophage recruitment into the cochlea and promotes the survival of spiral ganglion neurons after selective hair cell lesion. *J Neurosci* **35**: 15050–15061.
12. Ohgushi, H, Goldberg, VM and Caplan, AI (1989). Repair of bone defects with marrow cells and porous ceramic. Experiments in rats. *Acta Orthop Scand* **60**: 334–339.
13. Rickard, DJ, Sullivan, TA, Shenker, BJ, Leboy, PS and Kazhdan, I (1994). Induction of rapid osteoblast differentiation in rat bone marrow stromal cell cultures by dexamethasone and BMP-2. *Dev Biol* **161**: 218–228.
14. Ferrari, G, Cusella-De Angelis, G, Coletta, M, Paolucci, E, Stornaiuolo, A, Cossu, G *et al.* (1998). Muscle regeneration by bone marrow-derived myogenic progenitors. *Science* **279**: 1528–1530.
15. Mori, L, Bellini, A, Stacey, MA, Schmidt, M and Mattoli, S (2005). Fibrocytes contribute to the myofibroblast population in wounded skin and originate from the bone marrow. *Exp Cell Res* **304**: 81–90.
16. Bucala, R, Spiegel, LA, Chesney, J, Hogan, M and Cerami, A (1994). Circulating fibrocytes define a new leukocyte subpopulation that mediates tissue repair. *Mol Med* **1**: 71–81.
17. Lang, H, Ebihara, Y, Schmiedt, RA, Minamiguchi, H, Zhou, D, Smythe, N *et al.* (2006). Contribution of bone marrow hematopoietic stem cells to adult mouse inner ear: mesenchymal cells and fibrocytes. *J Comp Neurol* **496**: 187–201.
18. Kuijpers, W and Wilberts, DP (1976). The effect of ouabain and ethacrynic acid on ATPase activities in the inner ear of the rat and guinea pig. *ORL J Otorhinolaryngol Relat Spec* **38**: 321–327.

19. Wangemann, P and Marcus, DC (1992). The membrane potential of vestibular dark cells is controlled by a large Cl- conductance. *Hear Res* **62**: 149–156.
20. Hamada, M and Kimura, RS (1999). Morphological changes induced by administration of a Na+,K+-ATPase inhibitor in normal and hydropic inner ears of the guinea pig. *Acta Otolaryngol* **119**: 778–786.
21. Schmiedt, RA, Okamura, HO, Lang, H and Schulte, BA (2002). Ouabain application to the round window of the gerbil cochlea: a model of auditory neuropathy and apoptosis. *J Assoc Res Otolaryngol* **3**: 223–233.
22. Lang, H, Schulte, BA and Schmiedt, RA (2005). Ouabain induces apoptotic cell death in type I spiral ganglion neurons, but not type II neurons. *J Assoc Res Otolaryngol* **6**: 63–74.
23. Dao, MA and Nolta, JA (1999). Immunodeficient mice as models of human hematopoietic stem cell engraftment. *Curr Opin Immunol* **11**: 532–537.
24. Ito, M, Kobayashi, K, and Nakahata, T (2008). NOD/Shi-scid IL2rγnull (NOG) mice more appropriate for humanized mouse models. In: Nomura T, Watanabe T and Habu S (eds.). *Humanized Mice.* Springer. New York, NY pp. 53–76.
25. Shultz, LD, Ishikawa, F and Greiner, DL (2007). Humanized mice in translational biomedical research. *Nat Rev Immunol* **7**: 118–130.
26. Shultz, LD, Lyons, BL, Burzenski, LM, Gott, B, Chen, X, Chaleff, S *et al.* (2005). Human lymphoid and myeloid cell development in NOD/LtSz-scid IL2R gamma null mice engrafted with mobilized human hemopoietic stem cells. *J Immunol* **174**: 6477–6489.
27. Schafer, DP and Stevens, B (2015). Microglia Function in Central Nervous System Development and Plasticity. *Cold Spring Harb Perspect Biol* **7**: a020545.
28. Hess, DC, Abe, T, Hill, WD, Studdard, AM, Carothers, J, Masuya, M *et al.* (2004). Hematopoietic origin of microglial and perivascular cells in brain. *Exp Neurol* **186**: 134–144.
29. Hickey, WF and Kimura, H (1988). Perivascular microglial cells of the CNS are bone marrow-derived and present antigen in vivo. *Science* **239**: 290–292.
30. Priller, J, Flügel, A, Wehner, T, Boentert, M, Haas, CA, Prinz, M *et al.* (2001). Targeting gene-modified hematopoietic cells to the central nervous system: use of green fluorescent protein uncovers microglial engraftment. *Nat Med* **7**: 1356–1361.
31. Priller, J, Prinz, M, Heikenwalder, M, Zeller, N, Schwarz, P, Heppner, FL *et al.* (2006). Early and rapid engraftment of bone marrow-derived microglia in scrapie. *J Neurosci* **26**: 11753–11762.
32. Solomon, JN, Lewis, CA, Ajami, B, Corbel, SY, Rossi, FM and Krieger, C (2006). Origin and distribution of bone marrow-derived cells in the central nervous system in a mouse model of amyotrophic lateral sclerosis. *Glia* **53**: 744–753.
33. Tan, BT, Lee, MM and Ruan, R (2008). Bone-marrow-derived cells that home to acoustic deafened cochlea preserved their hematopoietic identity. *J Comp Neurol* **509**: 167–179.
34. Sera, Y, LaRue, AC, Moussa, O, Mehrotra, M, Duncan, JD, Williams, CR *et al.* (2009). Hematopoietic stem cell origin of adipocytes. *Exp Hematol* **37**: 1108–20, 1120.e1.
35. Juhn, SK and Rybak, LP (1981). Labyrinthine barriers and cochlear homeostasis. *Acta Otolaryngol* **91**: 529–534.
36. Juhn, SK, Rybak, LP and Prado, S (1981). Nature of blood-labyrinth barrier in experimental conditions. *Ann Otol Rhinol Laryngol* **90**(2 Pt 1): 135–141.
37. Larochelle, A, Bellavance, MA, Michaud, JP and Rivest, S (2016). Bone marrow-derived macrophages and the CNS: An update on the use of experimental chimeric mouse models and bone marrow transplantation in neurological disorders. *Biochim Biophys Acta* **1862**: 310–322.
38. Mildner, A, Schmidt, H, Nitsche, M, Merkler, D, Hanisch, UK, Mack, M *et al.* (2007). Microglia in the adult brain arise from Ly-6ChiCCR2+ monocytes only under defined host conditions. *Nat Neurosci* **10**: 1544–1553.
39. Lang, H, Li, M, Kilpatrick, LA, Zhu, J, Samuvel, DJ, Krug, EL *et al.* (2011). Sox2 up-regulation and glial cell proliferation following degeneration of spiral ganglion neurons in the adult mouse inner ear. *J Assoc Res Otolaryngol* **12**: 151–171.
40. Lang, H, Xing, Y, Brown, LN, Samuvel, DJ, Panganiban, CH, Havens, LT *et al.* (2015). Neural stem/progenitor cell properties of glial cells in the adult mouse auditory nerve. *Sci Rep* **5**: 13383.
41. Belema-Bedada, F, Uchida, S, Martire, A, Kostin, S and Braun, T (2008). Efficient homing of multipotent adult mesenchymal stem cells depends on FROUNT-mediated clustering of CCR2. *Cell Stem Cell* **2**: 566–575.
42. Heazlewood, SY, Oteiza, A, Cao, H and Nilsson, SK (2014). Analyzing hematopoietic stem cell homing, lodgment, and engraftment to better understand the bone marrow niche. *Ann N Y Acad Sci* **1310**: 119–128.
43. Hopman, RK and DiPersio, JF (2014). Advances in stem cell mobilization. *Blood Rev* **28**: 31–40.
44. Mehrotra, M, Williams, CR, Ogawa, M and LaRue, AC (2013). Hematopoietic stem cells give rise to osteo-chondrogenic cells. *Blood Cells Mol Dis* **50**: 41–49.
45. Ratajczak, MZ (2015). A novel view of the adult bone marrow stem cell hierarchy and stem cell trafficking. *Leukemia* **29**: 776–782.
46. Rogers, I, Yamanaka, N, Bielecki, R, Wong, CJ, Chua, S, Yuen, S *et al.* (2007). Identification and analysis of *in vitro* cultured CD45-positive cells capable of multi-lineage differentiation. *Exp Cell Res* **313**: 1839–1852.
47. Parakalan, R, Jiang, B, Nimmi, B, Janani, M, Jayapal, M, Lu, J *et al.* (2012). Transcriptome analysis of amoeboid and ramified microglia isolated from the corpus callosum of rat brain. *BMC Neurosci* **13**: 64.
48. Okano, T, Nakagawa, T, Kita, T, Kada, S, Yoshimoto, M, Nakahata, T *et al.* (2008). Bone marrow-derived cells expressing Iba1 are constitutively present as resident tissue macrophages in the mouse cochlea. *J Neurosci Res* **86**: 1758–1767.
49. Tornabene, SV, Sato, K, Pham, L, Billings, P and Keithley, EM (2006). Immune cell recruitment following acoustic trauma. *Hear Res* **222**: 115–124.
50. Jyothi, V, Li, M, Kilpatrick, LA, Smythe, N, LaRue, AC, Zhou, D *et al.* (2010). Unmyelinated auditory type I spiral ganglion neurons in congenic Ly5.1 mice. *J Comp Neurol* **518**: 3254–3271.
51. Sekerková, G, Zheng, L, Mugnaini, E and Bartles, JR (2008). Espin actin-cytoskeletal proteins are in rat type I spiral ganglion neurons and include splice-isoforms with a functional nuclear localization signal. *J Comp Neurol* **509**: 661–676.
52. Shi, X (2010). Resident macrophages in the cochlear blood-labyrinth barrier and their renewal via migration of bone-marrow-derived cells. *Cell Tissue Res* **342**: 21–30.
53. Hamann, J, Koning, N, Pouwels, W, Ulfman, LH, van Eijk, M, Stacey, M *et al.* (2007). EMR1, the human homolog of F4/80, is an eosinophil-specific receptor. *Eur J Immunol* **37**: 2797–2802.
54. Salzer, JL (1999). Creating barriers: a new role for Schwann cells and Desert hedgehog. *Neuron* **23**: 627–629.
55. Kilpatrick, LA, Zhu, J, Lee, FS and Lang, H (2011). Role of stromal cell-derived factor-1 expression in the injured mouse auditory nerve. *Otolaryngol Head Neck Surg* **145**: 1007–1015.
56. Schober, A, Karshovska, E, Zernecke, A and Weber, C (2006). SDF-1alpha-mediated tissue repair by stem cells: a promising tool in cardiovascular medicine? *Trends Cardiovasc Med* **16**: 103–108.
57. Lapidot, T, Dar, A and Kollet, O (2005). How do stem cells find their way home? *Blood* **106**: 1901–1910.
58. Ceradini, DJ, Kulkarni, AR, Callaghan, MJ, Tepper, OM, Bastidas, N, Kleinman, ME *et al.* (2004). Progenitor cell trafficking is regulated by hypoxic gradients through HIF-1 induction of SDF-1. *Nat Med* **10**: 858–864.
59. Lapidot, T (2001). Mechanism of human stem cell migration and repopulation of NOD/SCID and B2mnull NOD/SCID mice. The role of SDF-1/CXCR4 interactions. *Ann N Y Acad Sci* **938**: 83–95.
60. Dar, A, Kollet, O and Lapidot, T (2006). Mutual, reciprocal SDF-1/CXCR4 interactions between hematopoietic and bone marrow stromal cells regulate human stem cell migration and development in NOD/SCID chimeric mice. *Exp Hematol* **34**: 967–975.
61. Kollet, O, Peled, A, Byk, T, Ben-Hur, H, Greiner, D, Shultz, L *et al.* (2000). beta2 microglobulin-deficient (B2m(null)) NOD/SCID mice are excellent recipients for studying human stem cell function. *Blood* **95**: 3102–3105.
62. Fredelius, L and Rask-Andersen, H (1990). The role of macrophages in the disposal of degeneration products within the organ of corti after acoustic overstimulation. *Acta Otolaryngol* **109**: 76–82.
63. O'Halloran, EK and Oesterle, EC (2004). Characterization of leukocyte subtypes in chicken inner ear sensory epithelia. *J Comp Neurol* **475**: 340–360.
64. Hirose, K, Discolo, CM, Keasler, JR and Ransohoff, R (2005). Mononuclear phagocytes migrate into the murine cochlea after acoustic trauma. *J Comp Neurol* **489**: 180–194.
65. Peiser, L, Mukhopadhyay, S and Gordon, S (2002). Scavenger receptors in innate immunity. *Curr Opin Immunol* **14**: 123–128.
66. Silver, J, Schwab, ME and Popovich, PG (2015). Central nervous system regenerative failure: role of oligodendrocytes, astrocytes, and microglia. *Cold Spring Harb Perspect Biol* **7**: a020602.
67. Hines, DJ, Hines, RM, Mulligan, SJ and Macvicar, BA (2009). Microglia processes block the spread of damage in the brain and require functional chloride channels. *Glia* **57**: 1610–1618.
68. Lalancette-Hébert, M, Gowing, G, Simard, A, Weng, YC and Kriz, J (2007). Selective ablation of proliferating microglial cells exacerbates ischemic injury in the brain. *J Neurosci* **27**: 2596–2605.
69. Ceradini, DJ and Gurtner, GC (2005). Homing to hypoxia: HIF-1 as a mediator of progenitor cell recruitment to injured tissue. *Trends Cardiovasc Med* **15**: 57–63.
70. Claps, CM, Corcoran, KE, Cho, KJ and Rameshwar, P (2005). Stromal derived growth factor-1alpha as a beacon for stem cell homing in development and injury. *Curr Neurovasc Res* **2**: 319–329.
71. Ehrhardt, J and Morgan, J (2005). Regenerative capacity of skeletal muscle. *Curr Opin Neurol* **18**: 548–553.
72. Harris, JR, Brown, GA, Jorgensen, M, Kaushal, S, Ellis, EA, Grant, MB *et al.* (2006). Bone marrow-derived cells home to and regenerate retinal pigment epithelium after injury. *Invest Ophthalmol Vis Sci* **47**: 2108–2113.
73. Cesselli, D, Beltrami, AP, Rigo, S, Bergamin, N, D'Aurizio, F, Verardo, R *et al.* (2009). Multipotent progenitor cells are present in human peripheral blood. *Circ Res* **104**: 1225–1234.
74. Okabe, M, Ikawa, M, Kominami, K, Nakanishi, T and Nishimune, Y (1997). 'Green mice' as a source of ubiquitous green cells. *FEBS Lett* **407**: 313–319.
75. Ishikawa, F, Livingston, AG, Minamiguchi, H, Wingard, JR and Ogawa, M (2003). Human cord blood long-term engrafting cells are CD34+ CD38-. *Leukemia* **17**: 960–964.
76. Minamiguchi, H, Ishikawa, F, Fleming, PA, Yang, S, Drake, CJ, Wingard, JR *et al.* (2008). Transplanted human cord blood cells generate amylase-producing pancreatic acinar cells in engrafted mice. *Pancreas* **36**: e30–e35.
77. Minamiguchi, H, Wingard, JR, Laver, JH, Mainali, ES, Shultz, LD and Ogawa, M (2005). An assay for human hematopoietic stem cells based on transplantation into nonobese diabetic recombination activating gene-null perforin-null mice. *Biol Blood Marrow Transplant* **11**: 487–494.